

## Turbulent Annular Seals

In an annular seal, the flows are usually turbulent because of the high Reynolds numbers at which they

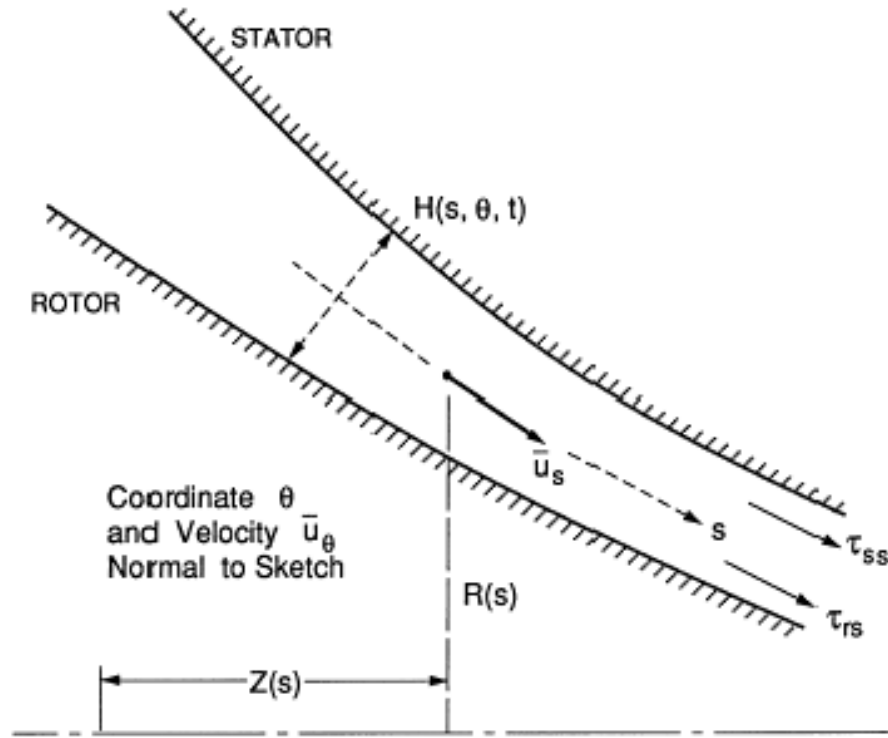


Figure 1: Sketch of fluid filled annulus between a rotor and a stator for turbulent lubrication analysis.

operate. In this section we describe the approaches taken to identify the rotordynamic properties of these flows. Black and his co-workers (Black 1969, Black and Jensen 1970) were the first to attempt to identify and model the rotordynamics of turbulent annular seals. Bulk flow models (similar to those of Reynolds lubrication equations) were used. These employ velocity components,  $\bar{u}_z(z, \theta)$  and  $\bar{u}_\theta(z, \theta)$ , that are averaged over the clearance. Black and Jensen used several heuristic assumptions in their model, such as the assumption that  $\bar{u}_\theta = R\Omega/2$ . Moreover, their governing equations do not reduce to recognizable turbulent lubrication equations. These issues caused Childs (1983b) to publish a revised version of the bulk flow model and we will focus on Childs' model here. Childs (1987, 1989) has also employed a geometric generalization of the same bulk flow model to examine the rotordynamic characteristics of discharge-to-suction leakage flows around shrouded centrifugal pump impellers, and it is therefore convenient to include here the more general form of his analysis. The geometry is sketched in figure 1, and is described by coordinates of the meridian of the gap as given by  $Z(s)$  and  $R(s)$ ,  $0 < s < L$ , where the coordinate,  $s$ , is measured along that meridian. The clearance is denoted by  $H(s, \theta, t)$  where the unperturbed value of  $H$  is  $\delta(s)$ . The equations governing the bulk flow are averaged over the clearance. This leads to a continuity equation of the form

$$\frac{\partial H}{\partial t} + \frac{\partial}{\partial s} (H\bar{u}_s) + \frac{1}{R} \frac{\partial}{\partial \theta} (H\bar{u}_\theta) + \frac{H}{R} \frac{dR}{ds} \bar{u}_s = 0 \quad (\text{Mcg1})$$

where  $\bar{u}_s$  and  $\bar{u}_\theta$  are velocities averaged over the local clearance. The meridional and circumferential

momentum equations are

$$-\frac{1}{\rho} \frac{\partial p}{\partial s} = \frac{\tau_{ss}}{\rho H} + \frac{\tau_{sr}}{\rho H} - \frac{\bar{u}_\theta^2}{R} \frac{dR}{ds} + \frac{\partial \bar{u}_s}{\partial t} + \frac{\bar{u}_\theta}{R} \frac{\partial \bar{u}_s}{\partial \theta} + \bar{u}_s \frac{\partial \bar{u}_s}{\partial \theta} \quad (\text{Mcg2})$$

$$-\frac{1}{\rho R} \frac{\partial p}{\partial \theta} = \frac{\tau_{\theta s}}{\rho H} + \frac{\tau_{\theta r}}{\rho H} + \frac{\partial \bar{u}_\theta}{\partial t} + \frac{\bar{u}_\theta}{R} \frac{\partial \bar{u}_\theta}{\partial \theta} + \bar{u}_s \frac{\partial \bar{u}_\theta}{\partial s} + \frac{\bar{u}_\theta \bar{u}_r}{R} \frac{dR}{ds} \quad (\text{Mcg3})$$

The approach used by Hirs (1973) is employed to determine the turbulent shear stresses,  $\tau_{ss}$  and  $\tau_{\theta s}$ , applied to the stator by the fluid in the  $s$  and  $\theta$  directions respectively:

$$\frac{\tau_{ss}}{\rho \bar{u}_s} = \frac{\tau_{\theta s}}{\rho \bar{u}_\theta} = \frac{A_s \bar{u}_s}{2} [1 + (\bar{u}_\theta / \bar{u}_s)^2]^{\frac{m_s+1}{2}} (Re_s)^{m_s} \quad (\text{Mcg4})$$

and the stresses,  $\tau_{sr}$  and  $\tau_{\theta r}$ , applied to the rotor by the fluid in the same directions:

$$\frac{\tau_{sr}}{\rho \bar{u}_s} = \frac{\tau_{\theta r}}{\rho(\bar{u}_\theta - \Omega R)} = \frac{A_r \bar{u}_s}{2} [1 + \{(\bar{u}_\theta - \Omega R) / \bar{u}_s\}^2]^{\frac{m_\theta+1}{2}} (Re_s)^{m_\theta} \quad (\text{Mcg5})$$

where the local meridional Reynolds number

$$Re_s = H \bar{u}_s / \nu \quad (\text{Mcg6})$$

and the constants  $A_s$ ,  $A_r$ ,  $m_s$  and  $m_\theta$  are chosen to fit the available data on turbulent shear stresses. Childs (1983a) uses typical values of these constants

$$A_s = A_r = 0.0664 ; m_s = m_\theta = -\frac{1}{4} \quad (\text{Mcg7})$$

The clearance, pressure, and velocities are divided into mean components (subscript 0) that would pertain in the absence of whirl, and small, linear perturbations (subscript 1) due to an eccentricity,  $\epsilon$ , rotating at the whirl frequency,  $\omega$ :

$$\begin{aligned} H(s, \theta, t) &= H_0(s) + \epsilon Re \{ H_1(s) e^{i(\theta - \omega t)} \} \\ p(s, \theta, t) &= p_0(s) + \epsilon Re \{ p_1(s) e^{i(\theta - \omega t)} \} \\ \bar{u}_s(s, \theta, t) &= \bar{u}_{s0}(s) + \epsilon Re \{ \bar{u}_{s1}(s) e^{i(\theta - \omega t)} \} \\ \bar{u}_\theta(s, \theta, t) &= \bar{u}_{\theta 0}(s) + \epsilon Re \{ \bar{u}_{\theta 1}(s) e^{i(\theta - \omega t)} \} \end{aligned} \quad (\text{Mcg8})$$

These expressions are substituted into the governing equations listed above to yield a set of equations for the mean flow quantities ( $p_0$ ,  $\bar{u}_{s0}$ , and  $\bar{u}_{\theta 0}$ ), and a second set of equations for the perturbation quantities ( $p_1$ ,  $\bar{u}_{s1}$ , and  $\bar{u}_{\theta 1}$ ); terms which are of quadratic or higher order in  $\epsilon$  are neglected.

With the kind of complex geometry associated, say, with discharge-to-suction leakage flows in centrifugal pumps, it is necessary to solve both sets of equations numerically in order to evaluate the pressures, and then the forces, on the rotor. However, with the simple geometry of a plain, untapered annular seal where

$$R(s) = R, H_0(s) = \delta, s = z, H_1(s) = 1 \quad (\text{Mcg9})$$

and in which

$$\bar{u}_{s0} = \frac{Q}{2\pi R \delta} = V \quad (\text{Mcg10})$$

where  $Q$  is the volumetric flow rate, Childs (1983a) was able to obtain analytic solutions to both the mean and perturbation equations. The resulting evaluation of the rotordynamic forces leads to the following rotordynamic coefficients:

$$K = \left( \frac{2\Delta p^T}{\rho V^2} \right) \phi^2 \frac{R}{2\lambda_1 L} [\mu_0 - \mu_2 (L/2\phi R)^2] \quad (\text{Mcg11})$$

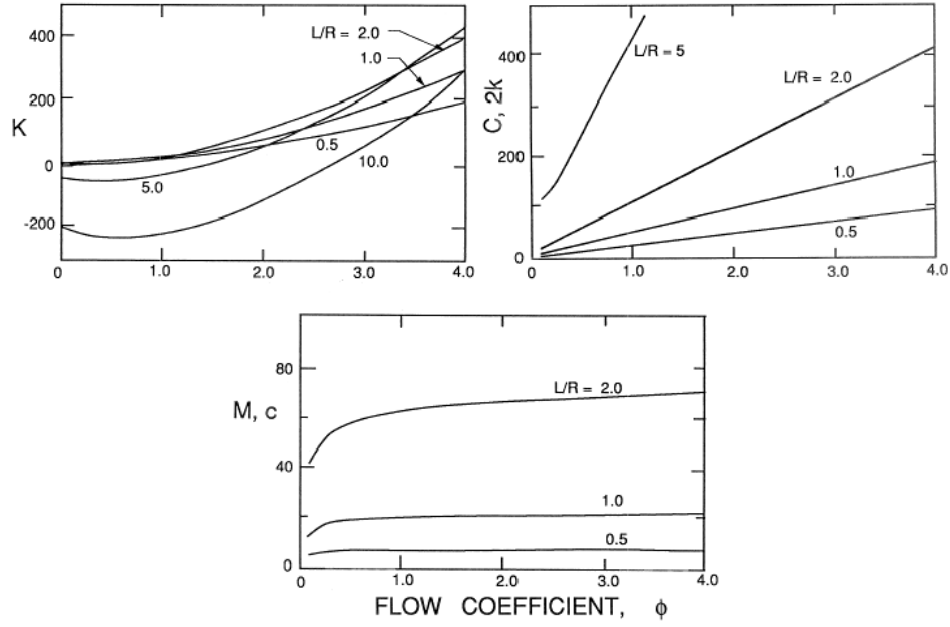


Figure 2: Typical dimensionless rotordynamic coefficients from Childs' (1983a) analysis of a plain, untapered and smooth annular seal with  $\delta/R = 0.01$ ,  $Re_V = 5000$ , and  $C_{EL} = 0.1$ .

$$C = 2k = \left( \frac{2\Delta p^T}{\rho V^2} \right) \frac{\phi \mu_1}{2\lambda_1} \quad (\text{Mcg12})$$

$$M = c = \left( \frac{2\Delta p^T}{\rho V^2} \right) \frac{\mu_2 L}{2\lambda_1 R} \quad (\text{Mcg13})$$

where  $\phi$  is the flow coefficient ( $\phi = V/\Omega R$ ), and  $\Delta p^T$  is the total pressure drop across the seal where

$$\frac{2\Delta p^T}{\rho V^2} = 1 + C_{EL}L + 2\lambda_2 \quad (\text{Mcg14})$$

and  $\lambda$ ,  $\mu_0$ ,  $\mu_1$ , and  $\mu_2$  are given by

$$\lambda_1 = 0.0664(Re_V)^{-\frac{1}{4}} \{1 + 1/4\phi^2\}^{\frac{3}{8}} \quad (\text{Mcg15})$$

$$\lambda_2 = \lambda_1 L/\delta \quad (\text{Mcg16})$$

$$\mu_0 = 5\lambda_2^2 \mu_5 / 2(1 + C_{EL} + 2\lambda_2) \quad (\text{Mcg17})$$

$$\mu_1 = 2\lambda_2 \left\{ \mu_5 + \frac{1}{2}\lambda_2 \mu_4 (\mu_5 + 1/6) \right\} / (1 + C_{EL} + 2\lambda_2) \quad (\text{Mcg18})$$

$$\mu_2 = \lambda_2 (\mu_5 + 1/6) / (1 + C_{EL} + 2\lambda_2) \quad (\text{Mcg19})$$

$$\mu_4 = (1 + 7\phi^2) / (1 + 4\phi^2) \quad (\text{Mcg20})$$

$$\mu_5 = (1 + C_{EL}) / 2(1 + C_{EL} + \mu_4 \lambda_2) \quad (\text{Mcg21})$$

where  $C_{EL}$  is an entrance loss coefficient for which the data of Yamada (1962) was used. Note that there are two terms in  $K$ ; the first, which contains  $\mu_0$ , results from the Lomakin effect, while the second, involving  $\mu_2$ , results from the Bernoulli effect (section (Nld)).

The results obtained by Black and Jensen (1970) are similar to the above except for the expressions for some of the  $\lambda$  and  $\mu$  quantities. Childs (1983a) contrasts the two sets of expressions, and observes

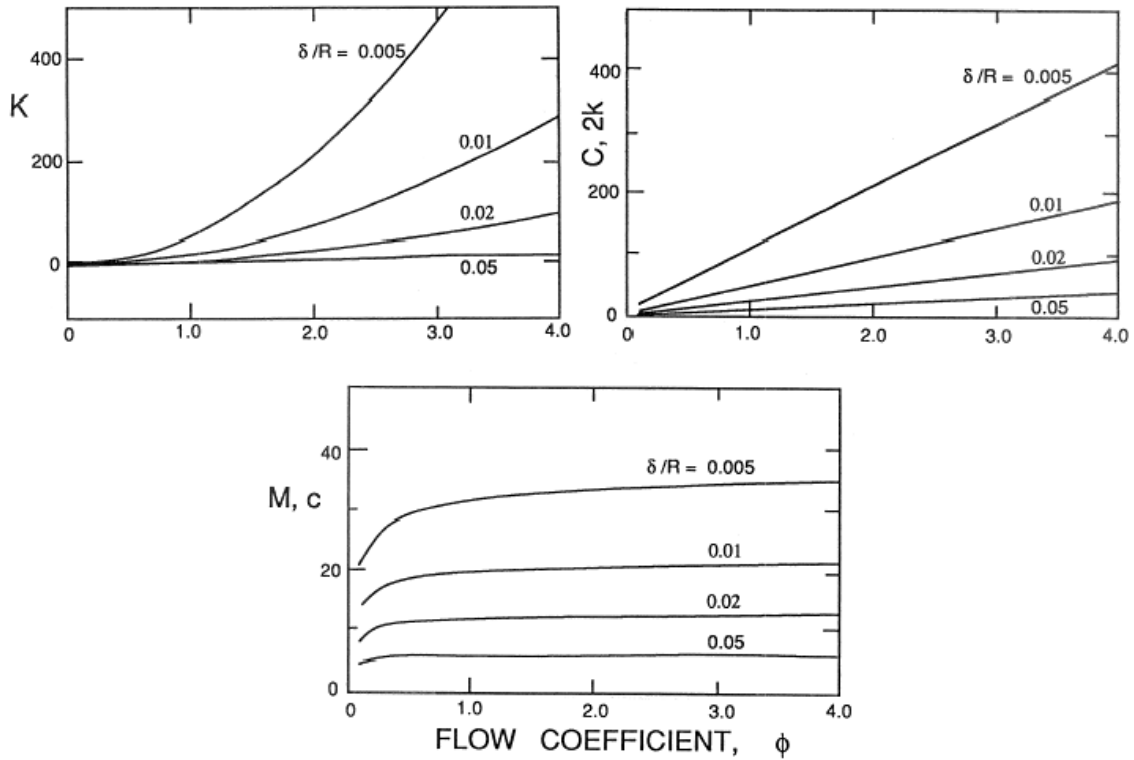


Figure 3: Typical dimensionless rotordynamic coefficients from Childs' (1983a) analysis of a plain, untapered and smooth annular seal with  $L/R = 1$ ,  $Re_V = 5000$ , and  $C_{EL} = 0.1$ .

that one of the primary discrepancies is that the Black and Jensen expressions yield a significant smaller added mass,  $M$ . We should also note that Childs (1983a) includes the effect of inlet preswirl which has a significant influence on the rotordynamic coefficients. Preswirl was not included in the results presented above.

Typical results from the expressions (Mcg11) to (Mcg13) are presented in figures 2 and 3, which show the variations with flow coefficient,  $\phi$ , and the geometric ratios,  $L/R$  and  $\delta/R$ . The effects of Reynolds number,  $Re_V$ , and of the entrance loss coefficient, are small as demonstrated in figure 4. Note the changes in sign in the direct stiffness,  $K$ , that result from the Lomakin effect becoming larger than the Bernoulli effect, or vice-versa. Note, also, that the whirl ratio,  $k/C$ , is 0.5 in all cases.

Childs and Dressman (1982) have published experimental measurements of the rotordynamic forces in a plain, smooth, annular seal with a length,  $L$ , to radius,  $R$ , ratio of 1.0, a clearance,  $\delta$ , to radius ratio of 0.01 at various flow rates and speeds. The excitation was synchronous ( $\omega/\Omega = 1$ ) so that

$$F_n = M - c - K \quad ; \quad F_t = -m - C + k \quad (\text{Mcg22})$$

Consequently, if one assumes the theoretical results  $M = c$ ,  $m = 0$  and  $C = 2k$  to be correct, then

$$F_n = -K \quad ; \quad F_t = -k = -\frac{c}{2} \quad (\text{Mcg23})$$

The data of Childs and Dressman for Reynolds numbers in the ranges  $2205 < Re_V < 13390$  and  $2700 < Re_\Omega < 10660$  are plotted in figure 4. It is readily seen that, apart from the geometric parameters  $L/R$  and  $\delta/R$ , the rotordynamic characteristics are primarily a function of the flow coefficient,  $\phi$ , defined as  $\phi = V/\Omega R = Re_V/Re_\Omega$ , and only depend weakly on the Reynolds number itself. The results from Childs' (1983a) theory using equations (Mcg11) to (Mcg13) are also shown and exhibit quite good agreement with the measurements. As can be seen, the theoretical results are also only weakly dependent on  $Re_V$  or the entrance loss coefficient,  $C_{EL}$ .

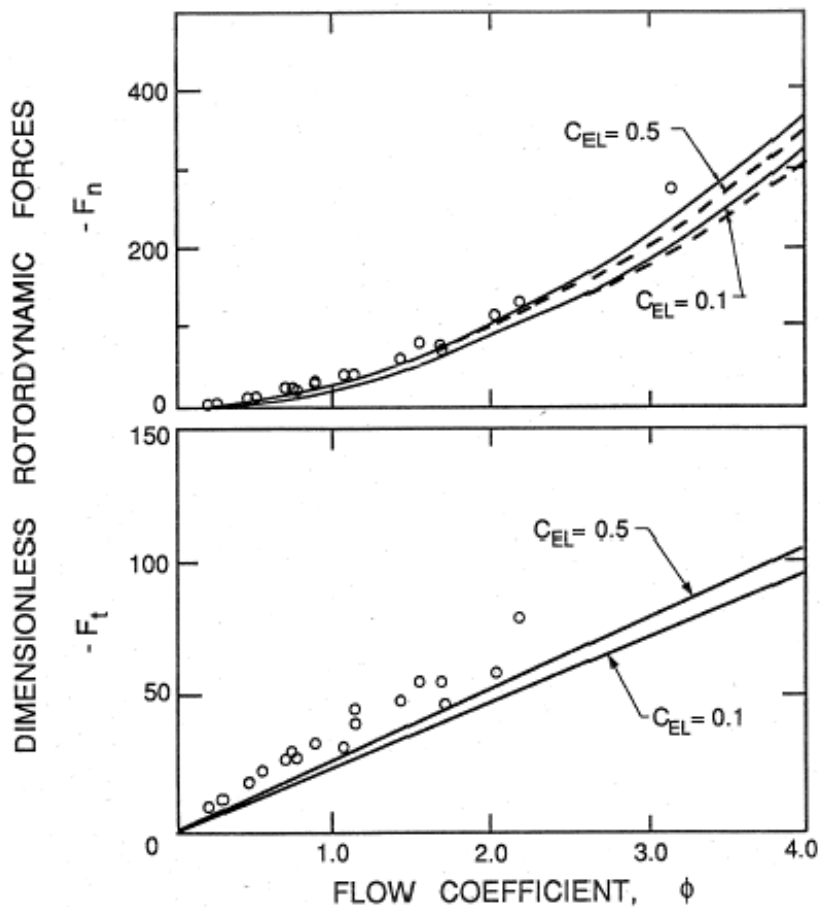


Figure 4: The measurements by Childs and Dressman (1982) of the rotordynamic forces for a straight, smooth annular seal ( $L/R = 1.0, \delta/R = 0.01$ ) for a range of Reynolds numbers,  $2205 < Re_V < 13390$ , and under synchronous excitation. Also shown are the predictions of the theory of Childs (1983a) for  $Re_V = 10000$  (solid lines) and  $15000$  (dashed lines) and two different entrance loss coefficients,  $C_{EL}$ , as shown.

Nordmann and Massman (1984) conducted experiments on a similar plain annular seal with  $L/R = 1.67$  and  $\delta/R = 0.0167$ , and measured the forces for both synchronous and nonsynchronous excitation. Thus, they were able to extract the rotordynamic coefficients  $M$ ,  $C$ ,  $c$ ,  $K$ , and  $k$ . Their results for a Reynolds number,  $Re_V = 5265$ , are presented in figure 5, where they are compared with the corresponding predictions of Childs' (1983a) theory (using  $C_{EL} = 0.1$ ). In comparing theory and experiment, we must remember that the results are quite insensitive to Reynolds number, and the theoretical data does not change much with changes in  $C_{EL}$ . Some of the Nordmann and Massmann data exhibits quite a lot of scatter; however, with the notable exception of the cross-coupled stiffness,  $k$ , the theory is in good agreement with the data. The reason for the discrepancy in the cross-coupled stiffness is unclear. However, one must bear in mind that the theory uses correlations developed from results for nominally *steady* turbulent flows, and must be regarded as tentative until there exists a greater understanding of unsteady turbulent flows.

In the last decade, a substantial body of data has been accumulated on the rotordynamic characteristics of annular seals, particularly as regards such geometric effects as taper, various kinds of roughness, and the effects of labyrinths. We include here only a few examples. Childs and Dressman (1985) conducted both theoretical and experimental investigations of the effect of taper on the synchronous rotordynamic forces. They showed that the introduction of a taper increases the leakage and the direct stiffness,  $K^*$ , but decreases the other rotordynamic coefficients. An optimum taper angle exists with respect to both the direct stiffness and the ratio of direct stiffness to leakage. Childs and Kim (1985) have examined

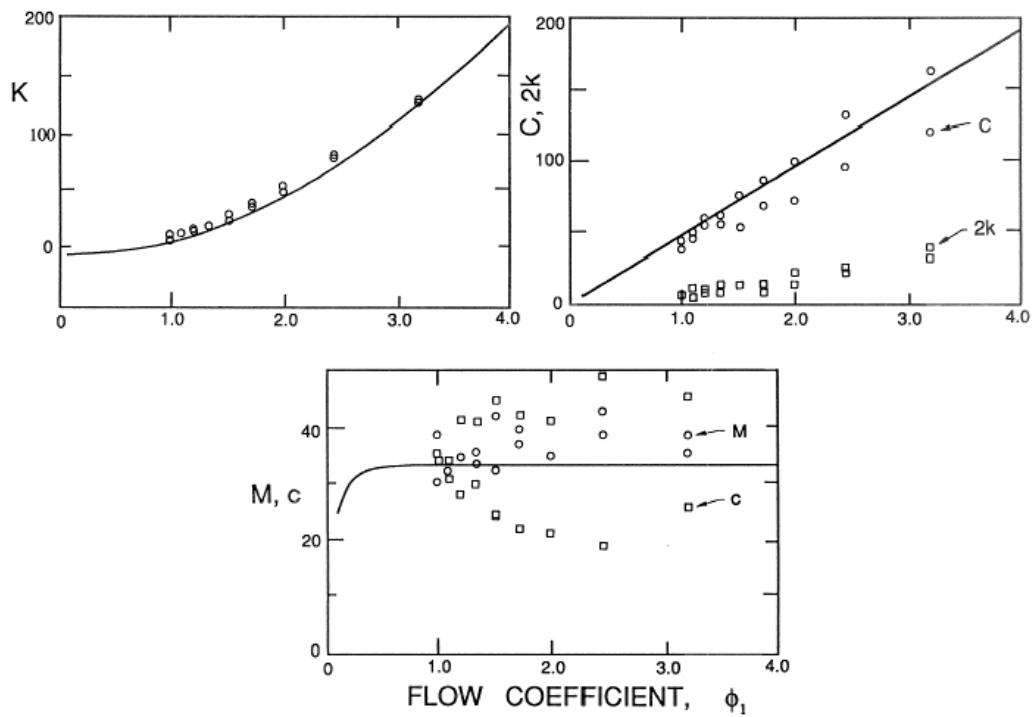


Figure 5: Dimensionless rotordynamic coefficients measured by Nordmann and Massmann (1984) for a plain seal with  $L/R = 1.67$ ,  $\delta/R = 0.0167$ , and  $Re_V = 5265$ . Also shown are the corresponding theoretical results using Childs' (1983a) theory with  $C_{EL} = 0.1$ .

the effects of directionally homogeneous surface roughness on both the rotor and the stator. Test results for four different surface roughnesses applied to the stator or casing (so-called "damper seals" that have smooth rotors) showed that the roughness increases the damping and decreases the leakage.